ORIGINAL RESEARCH

Nanoscaled hydrated antimony (V) oxide as a new approach to first-line antileishmanial drugs

Antonia MR Franco[1]
Iryna Grafova[2]
Fabiane V Soares[1,3]
Gennaro Gentile[4]
Claudia DC Wyrepkowski[1,3]
Marcos A Bolson[5]
Ézio Sargentini Jr[5]
Cosimo Carfagna[4]
Markku Leskelä[2]
Andriy Grafov[2]

[1]Laboratory of Leishmaniasis and Chagas Disease, National Institute of Amazonian Research (INPA), Manaus, Amazonas, Brazil; [2]Department of Chemistry, University of Helsinki, Helsinki, Finland; [3]Multi-Institutional Post-Graduate Program in Biotechnology, Federal University of Amazonas, Manaus, Amazonas, Brazil; [4]Institute for Polymers, Composites, and Biomaterials, National Research Council, Pozzuoli, Naples Province, Italy; [5]Laboratory of Environmental Chemistry, National Institute of Amazonian Research (INPA), Manaus, Amazonas, Brazil

Correspondence: Andriy Grafov
Department of Chemistry, University of Helsinki, A.I. Virtasen aukio I, 00014 University of Helsinki, Finland
Tel +358 2 9415 0221
Fax +358 2 9415 0198
Email andriy.grafov@helsinki.fi

Background: Coordination compounds of pentavalent antimony have been, and remain, the first-line drugs in leishmaniasis treatment for >70 years. Molecular forms of Sb (V) complexes are commercialized as sodium stibogluconate (Pentostam®) and meglumine antimoniate (MA) (Glucantime®). Ever-increasing drug resistance in the parasites limits the use of antimonials, due to the low drug concentrations being administered against high parasitic counts. Sb^{5+} toxicity provokes severe side effects during treatment. To enhance therapeutic potency and to increase Sb (V) concentration within the target cells, we decided to try a new active substance form, a hydrosol of $Sb_2O_5 \cdot nH_2O$ nanoparticles (NPs), instead of molecular drugs.

Methodology/principal findings: $Sb_2O_5 \cdot nH_2O$ NPs were synthesized by controlled $SbCl_5$ hydrolysis in a great excess of water. $Sb_2O_5 \cdot nH_2O$ phase formation was confirmed by X-ray diffraction. The surface of Sb (V) NPs was treated with ligands with a high affinity for target cell membrane receptors. The mean particle size determined by dynamic light scattering and transmission electron microscopy was ~35–45 nm. In vitro tests demonstrated a 2.5–3 times higher antiparasitic activity of Sb (V) nanohybrid hydrosols, when compared to MA solution. A similar comparison for in vivo treatment of experimental cutaneous leishmaniasis with Sb^{5+} nanohybrids showed a 1.75–1.85 times more effective decrease in the lesions. Microimages of tissue fragments confirmed the presence of NPs inside the cytoplasm of infected macrophages.

Conclusion/significance: $Sb_2O_5 \cdot nH_2O$ hydrosols are proposed as a new form of treatment for cutaneous leishmaniasis caused by *Leishmania amazonensis*. The NPs penetrate directly into the affected cells, creating a high local concentration of the drug, a precondition to overcoming the parasite resistance to molecular forms of pentavalent antimonials. The nanohybrids are more effective at a lower dose, when compared to MA, the molecular drug. Our data suggest that the new form of treatment has the potential to reduce and simplify the course of cutaneous leishmaniasis treatment. At the same time, $Sb_2O_5 \cdot nH_2O$ hydrosols provide an opportunity to avoid toxic antimony (V) spreading throughout the body.

Keywords: nanoparticle, leishmaniasis, hydrated antimony (V) oxide, TEM, transmission electron microscopy

Introduction

Leishmaniases are a group of diseases caused by protozoan parasites of the genus *Leishmania* transmitted to humans by the bites of infected female phlebotomine sandflies.[1] The World Health Organization (WHO) considers them to be neglected tropical diseases (NTDs). Cutaneous, mucocutaneous, and visceral leishmaniases affect 98 countries, with a prevalence of 12 million cases; 350 million people are at risk of infection.[2,3] There are no vaccines against these vector-borne diseases, and the clinical outcomes are described as ranging from a simple skin lesion to multi-organ failure, if untreated.[4] A new global strategy directed at eradication of NTDs by 2020

relies on a regular supply of quality-assured, cost-effective medicines and support from global partners.[5] To overcome the global impact of leishmaniases, the endemic countries need to provide an epidemiological surveillance system and insect vector control in order to reduce disease transmission and to improve earlier diagnosis and treatment.

For >70 years, coordination compounds of pentavalent antimony have been, and are still, the first-line drugs in South America, North Africa, Turkey, Bangladesh, and Nepal for the treatment of all forms of leishmaniasis. Coordination compounds of pentavalent antimony (molecular forms) are commercialized as sodium stibogluconate (Pentostam®) and meglumine antimoniate (MA) (Glucantime®). MA is one of the main commercial drugs based on pentavalent antimony; the Sb (V) concentration in MA solution is typically 81 mg/mL. The solution is administered as a course or repeated courses of intramuscular injections.

The mechanism of action of antimony is still unclear. Studies suggest that Sb (V) inhibits macromolecular biosynthesis in amastigotes (an intracellular form of the parasite in a vertebrate organism),[6] possibly altering metabolic processes by inhibiting glycolysis and fatty acid oxidation.[7] Other studies show that trivalent antimony Sb (III) causes disturbances in the thiol redox potential, which would lead to death of the parasite.[8] Antimonial treatment of leishmaniasis has been employed for decades, and parasite resistance to such treatment emerged over 20 years ago, first in the region of Bihar in India.[9] Ever-increasing drug resistance in the parasites limits the prolonged and effective use of antimonials, due to the low drug concentrations being administered in the presence of high parasitic counts. For this reason, the development of new dosage forms for drug delivery to parasite-infected cells is urgently needed. In addition, the toxicity of pentavalent antimony provokes severe side effects during the course of treatment.[10] Therefore, research activities should be focused on the minimization of such effects in the patients.

Recently, it became evident that drug development against leishmaniasis obligates a strengthening of the interaction between researchers developing in vivo models and experts in nanomaterials.[11] It has been emphasized in the literature that a lack of a multidisciplinary platform hampers the development of nanomedicine products and that development presumes a cross-fertilization at the highest level of knowledge between several different disciplines, including chemistry, nanotechnology, pharmacy, biology, and medicine, as a "must".[12–14] However, antileishmanial drugs are first intended for patients from the poorest regions of developing countries. Thus, according to WHO recommendations,

topical therapy of cutaneous and mucocutaneous forms of leishmaniasis will become increasingly important as it is less expensive and simple in application.[11]

Nanomedicine is an emerging multidisciplinary field that has a huge potential to restore the use of old state-of-the-art toxic drugs by modifying their bio-distribution, improving bioavailability, and reducing toxicity.[15] This valuable tool is able to cross biological barriers and is capable of meeting the challenge of killing the parasite inside the macrophage.[16] Liposomes, polymeric nanoparticles (NPs), metal NPs, and carbon-based materials are described in the literature as nanocarriers.[11] In any case, the question is about a specially developed nanocarrier loaded with an active substance in a molecular form. In other words, the influence of both the drug and the nanocarrier must be considered in the evaluation of the impact on the human body. The use of liposomes as carriers for the delivery of antimonials in cutaneous leishmaniasis treatment has been reported.[17] However, liposomes possess several limitations, such as instability that may lead to toxicity due to leakage of the drug into the bloodstream.[18] To the best of our knowledge, no other type of the abovementioned nanocarriers has ever been used for Sb^{5+} drug delivery.

In order to enhance the therapeutic potency of the existing drug, an increase of the Sb (V) concentration within the target cells was needed. We decided to try a new form of a known active substance: a hydrosol of Sb^{5+} containing NPs instead of the molecular drug form. In this case, we were not dealing with the loading of a medicine on a tailor-made NP, but with the synthesis of the NP, which is a drug itself. We succeed in synthesizing Sb (V) NPs that were surface treated and stabilized by ligands able to target receptors expressed on the cell membrane. The biological in vitro and in vivo tests demonstrated a high efficiency of the Sb^{5+} nanohybrids against cutaneous leishmaniasis.

Materials and methods
Synthesis of antimony (V) NPs

Ultra-high-purity freshly deionized water was used throughout the experiments. The synthesis was realized by a careful hydrolysis of $SbCl_5$ in a great molar excess of water, according to a procedure developed by us.[19] The transparent or slightly turbid sols obtained were purified by dialysis until they were essentially chloride free. The dialysis was performed in water, using cellulose membrane tubing (Sigma-Aldrich Co., product no D9777) according to standard procedures. Purified sols were then treated with an aqueous solution of either N-methylglucamine (NMGA) or panthenol and left overnight at room temperature under gentle stirring.

Antimony assay

Instrumentation

Antimony determination was performed on an atomic absorption spectrometer, SIMAA 6000 (PerkinElmer, Norwalk, CT, USA), using electrothermal atomization in a graphite furnace with a THGA tube and a Lumina™ multi-element hollow cathode lamp (both from PerkinElmer). The measurements were performed at the wavelength (λ) 217.6 nm. A slit width of 0.7 nm and a flushing gas flow rate of 250 mL/min were selected, according to the manufacturer's guidelines.

Procedure

All solutions were prepared using high-purity deionized water (ρ=18.2 MΩ·cm, Purelab Ultra, ELGA). Nitric acid (65% Suprapur®; Merck) was used for the preparation of all acidic solutions. Analytical calibration solutions containing 10, 20, 40, and 100 µg/L of Sb were prepared by serial dilutions of the analytical standard solution for atomic absorption, Titrisol® (Merck), containing 1,000 µg/L of Sb in 0.1% v/v HNO_3. The sample solutions were diluted 20,000–40,000 times with 1% v/v HNO_3.

A quantity of 20 µL of solution was injected into the furnace for analysis, both for the calibration and for the sample solutions; 5 µL of $Pd(NO_3)_2$ and $Mg(NO_3)_2$ solutions containing 5 and 3 µg of M^{2+}, respectively, were added as chemical modifiers. The same procedure was used for the calibration solutions as well. The heating program of the furnace developed for Sb analysis in serum and urine was optimized as shown in Table 1.

NP characterization

Dynamic light scattering (DLS)

Particle size and ζ-potential measurements were performed with a Zetasizer Nano (Malvern Instruments) using the original Sb^{5+} hydrosols in appropriate polystyrene cuvettes.

Transmission electron microscopy (TEM)

TEM micrographs were obtained with a FEI Tecnai G12 Spirit-Twin transmission electron microscope with a LaB_6

Table 1 Heating program for the Sb assay using electrothermal atomic absorption spectrometry with Pd^{2+} and Mg^{2+} as modifiers

Stage	Temperature (°C)	Ramp time (s)	Holding time (s)	Ar flow rate (mL/min)
1	110	1	30	250
2	130	15	30	250
3	1,300	10	20	250
4	2,300	0	5	0
5	2,500	1	3	250

source and operating with an acceleration voltage of 120 kV, equipped with a bottom-mounted FEI Eagle-4k CCD camera (Eindhoven, the Netherlands).

X-ray diffraction (XRD)

The XRD patterns were recorded on an X'Pert PRO MPD instrument (PANalytical B.V., the Netherlands) operating at 40 kV, 40 mA, using Cu-Kα radiation (λ=0.15418 nm), equipped with a built-in goniometer, an automatic divergence slit, and a PIXcel detector unit. Diffractograms were collected from 2θ=4 to 70°, using steps of 0.02°.

Parasite culture

The promastigote culture of a Brazilian *Leishmania* strain (*Leishmania (Leishmania) amazonensis*) was obtained from the collection of the Leishmaniasis and Chagas Disease Laboratory, National Institute of Amazonian Research (INPA; MHOM/09/BR/IM5584). The strain was maintained in an NNN- (Novy, MacNeal, and Nicolle) modified blood agar base (BD Biosciences, USA) supplemented with Roswell Park Memorial Institute (RPMI)-1640 (Sigma, USA, R-7388), with 20 mM HEPES and L-glutamine without $NaHCO_3$ at 25°C. *Leishmania* promastigotes were cultured in a sterile 25 cm² tissue culture flask containing RPMI-1640 medium supplemented with 10% of heat-inactivated fetal bovine serum (iFBS) (Biobras, Brazil) at pH =7.2 and at a temperature of 25°C. The parasites were centrifuged at 4,000 rpm for 10 min, diluted with sterile RPMI-1640, and counted using a Neubauer chamber viewed under an optical microscope. Then, the parasites were diluted with fresh complete medium to a concentration of 2×10^6 cells/mL.

Leishmanicidal activity in vitro

Promastigotes of *L. amazonensis* were cultivated and amplified in a modified NNN biphasic medium using sterile phosphate-buffered saline (PBS). Parasites at the end of log phase (beginning of the stationary phase) were centrifuged at 4,500 rpm for 10 min, washed three times with PBS, and centrifuged at the same speed for 10 min. The parasite suspension was diluted with fresh culture medium to a final concentration of 2×10^6 cells/mL.

The tests were performed in a sterile transparent polystyrene 96-well cell culture plate using a maximum volume of 200 µL of the test solution per well. A volume of 100 µL of culture medium and 100 µL of the Sb (V) NP hydrosol were added in wells of the first column (except for the last two rows), and serial 1:2 v/v dilution of that

mixture with the culture medium was carried out into the subsequent columns.

Two hydrosol samples, VRSb$_1$ and VRSb$_2$, were used in the in vitro experiments. Both contained the NMGA ligand, but the VRSb$_2$ was less concentrated for Sb^{5+}. Thus, Sb^{5+} concentrations ranging from 4.21 to 0.27 mg/mL and from 1.77 to 0.11 mg/mL were obtained for VRSb$_1$ and VRSb$_2$ samples, respectively. Subsequently, 100 µL of cultured parasite suspension (2×10^6 cells/mL) was added to each well of the plate. The plate was incubated at 25°C for 48 h, and the number of viable parasite cells in each well was determined microscopically by Trypan blue (Sigma) dye exclusion test in a Neubauer hemocytometric chamber. The last two rows were left for negative control (NC) and positive control. One NC received the culture medium with ligands and the other one the medium only, while the positive control contained serial dilutions of the commercial antileishmanial drug MA solution. All experiments were performed in triplicate.

Antileishmanial efficacy calculation
The percentage efficacy (%E) was calculated using the formula

$$\%E = \frac{\bar{x}_{NCG} - \bar{x}_{TG}}{\bar{x}_{NCG}} \times 100\%,$$

where $\bar{x}_{NCG}$ and $\bar{x}_{TG}$ are arithmetic means of the number of viable parasites in the NC group and the treated group, respectively.[20]

Leishmanicidal activity in vivo
Adult male Syrian hamsters (*Mesocricetus auratus*) were selected as a biological model and maintained under pathogen-free conditions in the Bioterium (Laboratory Animal Facility) of the INPA (National Institute of Amazonian Research). They were inoculated into the snout with 10^6 cells/mL of the stationary-phase promastigote form of *L. amazonensis* parasite.

Three groups of five experimental animals each received a treatment of the Sb-NP formulas (VVSb$_1$ and VVSb$_2$) or of commercial MA (4.4 mg/kg/day of MA; Aventis, Brazil). The fourth, NC, group did not receive any chemotherapy. The MA was administered by the intramuscular route; other treatments were applied intralesionally once daily with the same amount of 0.4 mL (for VVSb$_1$ [Sb^{5+}] =4.09 mg/mL/day, for VVSb$_2$ [Sb^{5+}] =0.65 mg/mL/day). The VVSb$_1$ sample contained the Sb^{5+} NPs treated with NMGA ligand, and the VVSb$_2$ was treated with panthenol. The total lesion size was derived from the mean lesion length, width, and height

measured and recorded daily with a digital Vernier caliper (Precision Zaas/Amatools).

The treatment lasted for 26 days (20 follow-up days with 3 weekly intervals of 2 days). Subsequently, the animals were euthanized and necropsy was performed. Fragments of the lesion tissues were inoculated in NNN biphasic culture medium and complete RPMI-1640 cell culture medium (Sigma) supplemented with 10% of iFBS to determine the parasite viability.

Tissue sample preparation for TEM investigation
Fragments of the lesion tissues were fixed in 2.5% glutaraldehyde and 0.1 M cacodylate buffer and dehydrated through a series of treatments in solutions at increasing acetone concentrations (10, 30, 60, 90, and 100% by volume). Each treatment lasted for 15 min, and the last 100% acetone treatment was repeated three times. Dehydrated samples were embedded into epoxy resin 45359 (Epoxy-Embedding Kit; Fluka) according to standard protocols. The impregnation process was performed in three steps. First, the samples were treated with acetone/epoxy mixture (1:1 v/v) for 30 min, then with acetone/epoxy mixture (1:2 v/v) for a further 30 min. Subsequently, the samples were immersed in a final epoxy mixture and transferred to a silicone rubber mold. Polymerization of the epoxy resin was performed at 45°C for 48 h. The embedded samples were then ultrasectioned at room temperature on a Leica EM UC6/FC6 ultramicrotome at a speed of 1–2 mm/s. Ultrathin sections with a thickness of 80–90 nm were produced, collected, and mounted on 400-mesh copper grids.

Ethical approval
All experiments were performed strictly following the recommendations of the Guide for the Care and Use of Laboratory Animals of the Brazilian National Council of Animal Experimentation (COBEA). The ethical permission protocols were approved by the Animal Ethics Committee of the National Institute for Amazonian Research (CEUA/INPA, no 011/2012 and no 009/2015).

Results and discussion
The original idea in this study was to obtain stable active NPs directly in a hydrosol form. We supposed that the nano-sized particles would penetrate directly into affected cells, creating a high local concentration of the drug. In this way, a stronger therapeutic effect could be achieved. At the same time, undesirable spreading of active substance throughout

the body could be avoided, thus reducing significantly several undesirable side effects.

The most suitable compound for forming Sb^{5+}-containing sols in water was the hydrated antimony (V) oxide, $Sb_2O_5 \cdot nH_2O$, also called polyantimonic acid. This material was obtained previously in a solid form for proton conducting and electrochromic applications.[21–25] All the cited papers deal with the solid material obtained by precipitation, consequent drying, and thermal treatment; thus, the particles involved were forced to aggregate and crystallize.

Our principal objective was to obtain a stable $Sb_2O_5 \cdot nH_2O$ hydrosol instead of a crystalline precipitate. For that purpose, the reaction was carried out at a high molar excess of water (1,000–2,500 mol H_2O:1 mol Sb) by slow dropwise addition of $SbCl_5$ at room temperature and effective stirring.[19]

$$2SbCl_5 + (5+n)H_2O = Sb_2O_5 \times nH_2O \downarrow + 10HCl$$
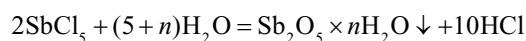
Use of the high excess of water prevented both heating of the reaction mixture due to the exothermic hydrolysis reaction and formation of a crystalline precipitate. The transparent or slightly turbid sols obtained were purified by dialysis from the HCl formed in the reaction. Purified sols

were then treated with an aqueous solution of either NMGA or panthenol and left overnight at room temperature under gentle stirring. The NMGA was chosen by analogy with the commercial drug MA, a solution of the Sb (V) coordination compound containing NMGA ligands.[26] 2,4-Dihydroxy-*N*-(3-hydroxypropyl)-3,3-dimethylbutanamide or panthenol (B5 provitamin) was used as another nitrogen-containing ligand. It is an effective skin penetration-enhancing agent that reduces skin inflammation and accelerates the healing rate of wounds.[27] Those ligands were chosen to stabilize the $Sb_2O_5 \cdot nH_2O$ NPs and to facilitate the drug uptake to cells by endocytosis. Finally, the hydrosols were allowed to evaporate in order to achieve Sb concentrations comparable with the Sb^{5+} content in MA diluted for use in experimental animals (20.25 mg/mL).

$Sb_2O_5 \cdot nH_2O$ NP sol possessed a very high stability, and it did not decompose or undergo modifications during storage under ambient conditions for >1 year. The mean particle size and ζ-potential were measured by DLS (Figure 1A and B) using the original Sb^{5+} hydrosols in appropriate polystyrene cuvettes. The NP size was also confirmed by TEM (Figure 1C). A part of the sol was allowed to dry, and X-ray diffractograms of the powder obtained were recorded. The diffraction pattern
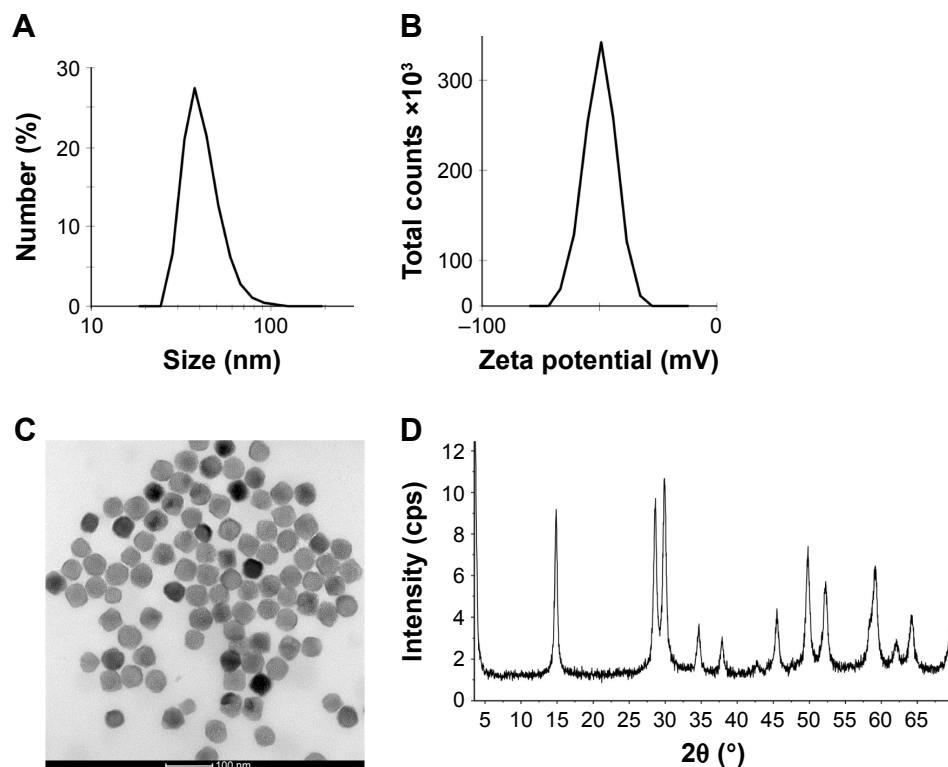

Figure 1 Characterization of NPs: particle size distribution (**A**) and ζ-potential (**B**) measured by DLS; TEM micrograph of the NPs (**C**); XRD pattern of a precipitate after drying of the hydrosol (**D**).
Abbreviations: NPs, nanoparticles; DLS, dynamic light scattering; TEM, transmission electron microscopy; XRD, X-ray diffraction.

of the material (Figure 1D) corresponded to that of hydrated antimony (V) oxide, $Sb_2O_5 \cdot nH_2O$.[24]

The distribution of particle size was quite narrow, and the maximum indicated a mean NP size of ~42 nm (Figure 1A). The magnitude of ζ-potential, −49.8 mV (Figure 1B), gives evidence of a very high stability of the sol due to effective electrostatic repulsion of the adjacent particles, which prevents their aggregation. The negative value of the ζ-potential reveals the anionic character of the NPs, intrinsic to the polyantimonic acid particles. A multitude of uniform nano-sized particles is clearly visible on the TEM micrograph (Figure 1C). The NPs had a regular shape and size of ~35–45 nm. The particle size and its distribution measured by DLS were in a good agreement with the TEM data.

The use of a nanoparticulated active ingredient in a hydrosol enables topical or intralesional drug administration. Such administration routes play an important role in dermatologic therapy, since they permit direct delivery of medication into skin lesions, the areas where the parasites are mostly concentrated. Such therapy could be particularly prominent for the treatment of the cutaneous form of leishmaniasis. In this way, the drug delivered into the dermis acts over a period of time, resulting in prolonged therapy. Simultaneously, the adverse effects of systemic therapy would be avoided or minimized.

The nanoparticulated hydrated antimony (V) oxide sols (samples $VRSb_1$ and $VRSb_2$) were, for the first time, tested in vitro in order to evaluate their antileishmanial activity against promastigote forms of the pathogenic protozoa *L. amazonensis*. Antimony concentrations in the hydrosols, determined by atomic absorption spectrometry, were as follows: [Sb] =16.87 mg/mL for $VRSb_1$ and [Sb] =7.10 mg/mL for $VRSb_2$. Stationary-phase promastigotes of *L. amazonensis* (10^6 cells/mL) were cultured at 25°C in RPMI-1640 medium supplemented with 10% iFBS and used for the experiments.

The antiparasitic activity was evaluated by viable cell counting after 24 and 48 h of the promastigotes being exposed to the test solutions versus positive control and NC ones. All the bioassays were done with serial dilutions (1:4 to 1:64) of substances, and each one was carried out in triplicate. The Sb^{5+} hydrosol to cell culture medium ratio (v/v) was 1:3 throughout all experiments. Thus, the maximum concentration of the $VRSb_1$ sample was 16.87:4=4.22 mg/mL. MA solution containing 20.25 mg/mL of Sb^{5+} was used as a positive control; this refers only to the presence of parasites in the same axenic culture medium at the experimental conditions used. An initial inoculum of the flagellates, 10^6 cells/mL, in axenic culture medium was used as an NC. Cells continued to grow, giving rise to a mean value of 1.7×10^6 cells/mL after 24 h and 2.9×10^6 cells/mL after 48 h. The experimental results are shown in Figure 2.

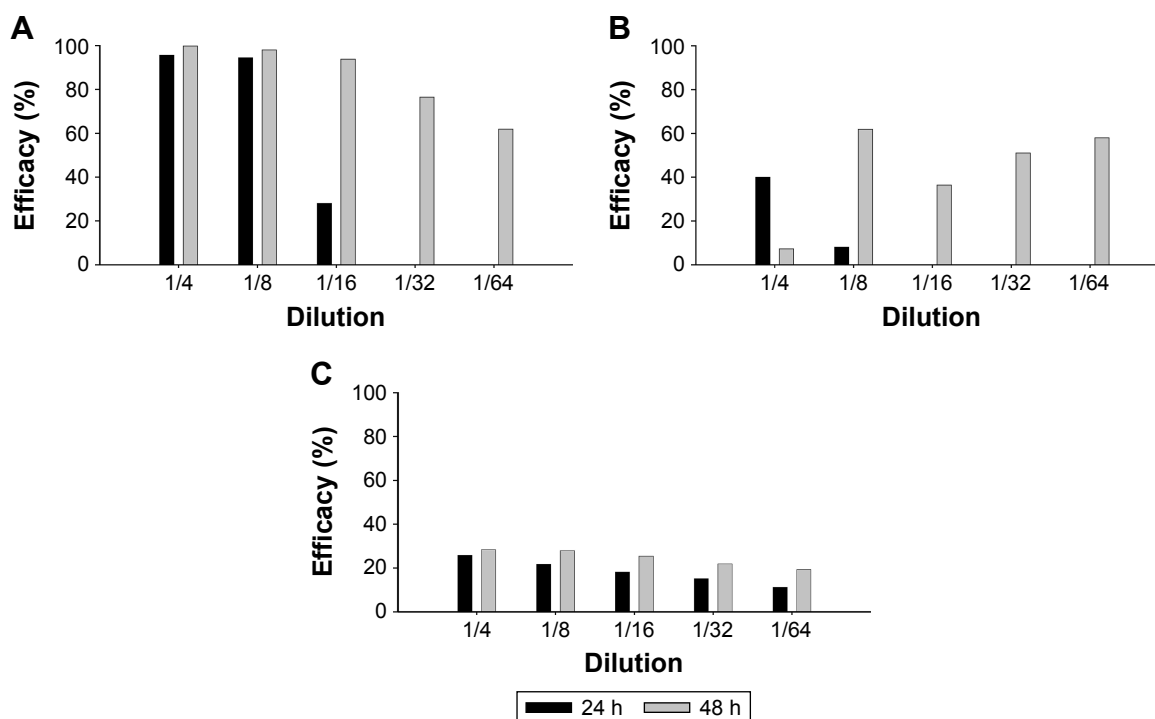**Figure 2** Percentage antileishmanial efficacy in vitro of $Sb_2O_5 \cdot nH_2O$ nanohybrids with NMGA, compared to MA at different dilutions after exposure for 24 and 48 h.
Notes: The graphs correspond to $VRSb_1$ (**A**), Sb^{5+} concentrations 4.22, 2.11, 1.05, 0.53, and 0.26 mg/mL; $VRSb_2$ (**B**), Sb^{5+} concentrations 1.78, 0.89, 0.44, 0.22, and 0.11 mg/mL; MA (**C**) Sb^{5+} concentrations 5.06, 2.53, 1.26, 0.63, and 0.32 mg/mL.
Abbreviations: NMGA, *N*-methylglucamine; MA, meglumine antimoniate.

As illustrated by the graph for the $VRSb_1$ sample (Figure 2A), ~100% efficacy was observed both after 24 h and after 48 h of the parasites being exposed to the hydrosols at Sb^{5+} concentrations of 4.22 and 2.11 mg/mL. After 48 h of exposure, the efficacy remained practically at the same level even for the second dilution (1:16) and slightly decreased at the subsequent dilutions. However, no visible activity was observed for the dilutions starting from 1:32 after 24 h of the experiment. The half maximal effective concentration (EC_{50}) values for $VRSb_1$ were found to be 1.35 mg/mL after 24 h of exposure and <0.26 mg/mL after 48 h. As can be seen from the graphs (Figure 2A and B), the efficacy after 24 h of exposure was registered only at higher concentrations for both NP hydrosol samples. $VRSb_2$ showed a weak inhibition effect after 24 h, and no visible activity was found for dilutions higher than 1:16. After 48 h, the EC_{50} was observed at 0.11 mg/mL, when compared with a mean number of viable parasites found in the NC. We would like to draw particular attention to the fact that both nanohybrid hydrosols revealed higher antiparasitic activity in vitro, when compared to the MA solution (positive control). The graph (Figure 2C) demonstrates that the EC_{50} level was never reached in the MA experiments.

Thus, the in vitro tests convincingly showed that the antiparasitic activity of Sb^{5+} nanohybrids is considerably higher (2.5–3 times) when compared to the commercial molecular form of the pentavalent antimonial drug. The maximum efficacy was observed after 48 h for $VRSb_1$ hydrosol, which was more concentrated for Sb (V) (Figure 2A).

The therapeutic action of the $Sb_2O_5 \cdot nH_2O$ nanohybrid solutions was studied in vivo in an animal model on experimental cutaneous leishmaniasis caused by the *L. amazonensis* parasite. Experiments were carried out on groups of adult male Syrian hamsters selected as the biological model and followed up by measurements of the skin lesion size, its evolution, and development in response to the treatment.

Each group of laboratory animals received one of the following treatments: $Sb_2O_5 \cdot nH_2O$ nanohybrids surface treated with NMGA ligand ($VVSb_1$); $Sb_2O_5 \cdot nH_2O$ nanohybrids surface treated with panthenol ligand ($VVSb_2$); and commercial MA solution. The MA was administered by the intramuscular route, whereas the other treatments were applied intralesionally once daily. The NC group did not receive any chemotherapy.

The results of the in vivo experiments are shown in Figure 3A as plots of mean lesion size for each day of treatment and lesion evolution trend lines. As illustrated by the graph, a more visible reduction of skin lesion size was observed in groups treated with $VVSb_1$ and $VVSb_2$

nanohybrids. Both the NC group and the group receiving molecular drug treatment (MA) exhibited higher lesion sizes with a tendency to grow. The latter became particularly evident during the second half of the treatment. During the first half of the treatment, the best size reduction tendency of the lesions provoked by *L. amazonensis* was observed for $VVSb_1$ nanohybrid hydrosol containing NMGA ligand (Figure 3A). In the second half of the treatment, the therapeutic efficiency of the panthenol-containing hydrosol $VVSb_2$ reached the same level as for $VVSb_1$ or even higher. This fact may be attributed to the known skin penetration enhancement property of the panthenol ligand.[28]

At the end of the treatment, the biggest mean lesion size was observed in the NC group. It was 1.31 times bigger than the mean lesion size in the group treated with the molecular drug (MA group) and 2.3–2.45 times bigger than those observed in both nanohybrid treatment-receiving groups ($VVSb_1$ and $VVSb_2$). The results of our in vivo experiments convincingly show the advantage of $Sb_2O_5 \cdot nH_2O$ nanohybrid treatment over the MA one: the nanoformulas were 1.75–1.85 times more efficient.

The abovementioned tendencies were also clearly confirmed by photographs (Figure 4) showing the lesion behavior on the snouts of hamsters experimentally infected with *L. amazonensis*. The images demonstrate the response to the treatment with $VVSb_1$ and $VVSb_2$ nanohybrids compared to that with the molecular antimonial drug (MA) and in an absence of treatment (NC). No clinical signs of toxicity were observed in animals receiving the treatments. The hamsters were of healthy appearance and retained mobility and vitality. Furthermore, the percentage of mortality was zero during the 26 days of treatment. At the very beginning of treatment, all animals presented nodular lesions of bulky appearance and uniform diameter. Differences began to appear throughout the experiment. The NC group had ulcerations without defined borders, intense edema, erythema, and crust appearance. The MA-treated group demonstrated a slight diminution of the skin lesion area, persistent ulceration, and crust emergence on the lesion border, whereas the groups of animals treated with both $VVSb_1$ and $VVSb_2$ NPs revealed a significant decrease of injury, a mild erythema, and/or skin scales.

In addition to lesion size measurements, tissue fragments from the lesion area were collected for TEM investigation and for detection of the occurrence of NPs inside the cells. TEM images clearly showed the microstructural features of the sequential tissue response after inoculation with *L. amazonensis* and treatment. Intracellular amastigote forms of the parasite were found at the inoculation site of the NC group. The presence of nanohybrids inside the
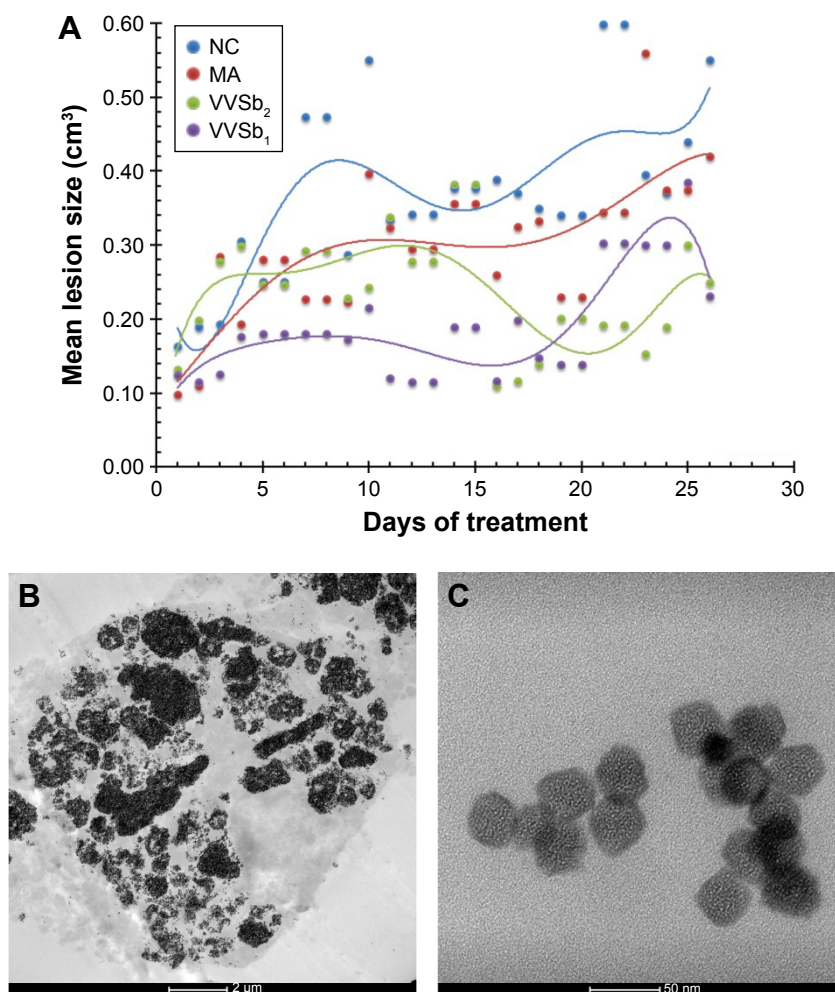
Figure 3 Scatter plots and trend lines of mean lesion size monitored in experimental animals infected with *Leishmania amazonensis* (**A**); TEM micrographs showing the presence of $Sb_2O_5 \cdot nH_2O$ NPs in the cytoplasm of a phagocyte of an animal treated with $VVSb_1$ (**B**); and those NPs visualized at a higher magnification (**C**).
Abbreviations: TEM, transmission electron microscopy; NPs, nanoparticles; NC, negative control; MA, meglumine antimoniate.

cytoplasm of the infected macrophages was observed for all the animals that had received treatment with $VVSb_1$ or $VVSb_2$ (Figure 3B and C). The amount of NPs in the tissue was dependent on the total dose of Sb^{5+} received during the treatment. An interesting tendency was observed for each hydrosol sample: the quantity of NPs inside the cytoplasm of infected macrophages decreased for the tissue samples extracted after 26 days of treatment with respect to those extracted after 15 days. Hence, the nanoparticulated drug was being metabolized. The abovementioned assumption was also supported by TEM. NPs of a mean size of 49.3–48.4 nm were found in the snout tissue cells from infected hamsters biopsied after 15 days of treatment, whereas those after 26 days were smaller in size (45.5–44.5 nm). It should also be noted that no amastigotes were found within the macrophages of treated animals, despite their positive re-isolation in the cell culture medium.

Conclusion

Nanoscaled hydrated antimony (V) oxide hydrosols are proposed as a new effective dosage form for topical treatment of experimental cutaneous leishmaniasis caused by *L. amazonensis*. The nanohybrids obtained differ from any previously made nano-sized drug forms, such as liposomes or nanocapsules containing the molecular form of the drug as a payload inside a nanoscaled vehicle. The novelty of the proposed approach consists of the fact that $Sb_2O_5 \cdot nH_2O$ NPs are drugs themselves; they are nanomatrices made of the active compound (Sb^{5+}), which may bear different targeting ligands as a nanohybrid component.

The high stability of the $Sb_2O_5 \cdot nH_2O$ hydrosols was established by ζ-potential measurements. The uniformity of the particles, as well as their size, was determined by DLS and TEM studies. In order to facilitate the receptor-mediated endocytosis of $Sb_2O_5 \cdot nH_2O$ NPs, targeting ligands NMGA and
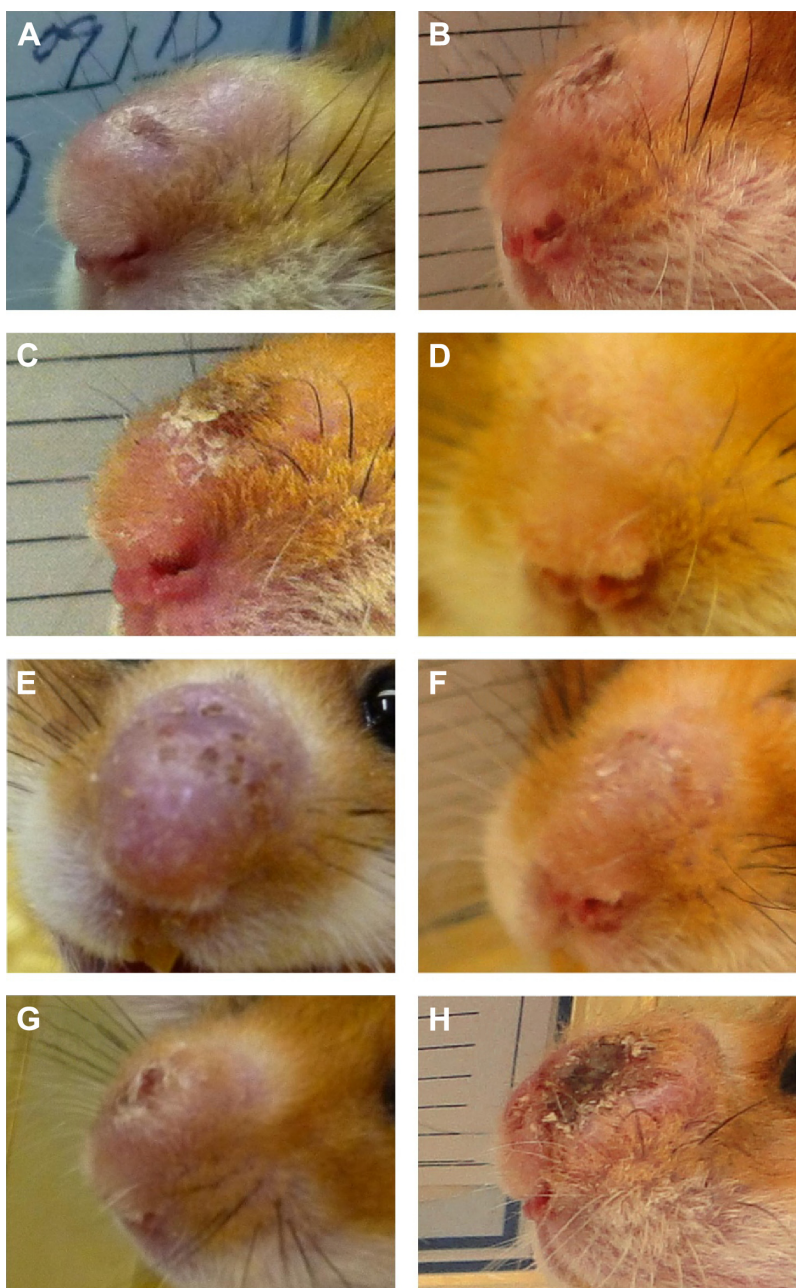
Figure 4 Clinical evolution of lesions on the snouts of hamsters (*Mesocricetus auratus*) experimentally infected with *Leishmania amazonensis* and monitored for 26 days.
Notes: MA-treated animals on the 5th (**A**) and 26th (**B**) days; VVSb₁-treated animals on the 5th (**C**) and 26th (**D**) days; VVSb₂-treated animals on the 5th (**E**) and 26th (**F**) days; untreated NC group animals on the 5th (**G**) and 26th (**H**) days.
Abbreviations: MA, meglumine antimoniate; NC, negative control.

panthenol were used for their surface treatment. In vitro tests were performed on promastigote forms of *L. amazonensis*. Sb (V) nanohybrids demonstrated 2.5–3 times higher antiparasitic activity, when compared to MA, a molecular drug form. Our in vivo data on the treatment of skin lesions provoked by experimental cutaneous leishmaniasis in hamsters (*M. auratus*) showed a 1.75–1.85 times higher efficacy of the nanohybrids with respect to MA. TEM images of tissue fragments confirmed the uptake of the pentavalent antimony NPs directly into the

affected cells, creating a high local concentration of the drug. The latter fact is a precondition to overcoming the resistance of the parasites to the molecular form of the medicine.

Furthermore, the nanohybrids were more effective at a lower administered dose when compared to the commercial first-choice molecular drug MA. The toxicological profile of the nanohybrids and new topical administration routes, as well as other $Sb_2O_5 \cdot nH_2O$ containing nanohybrid formulas, are now under development.

Acknowledgments

Disclosure

The authors report no conflicts of interest in this work.

References

1. World Health Organization [webpage on the Internet]. Leishmaniasis. Fact sheet; 2016. Available from: http://www.who.int/mediacentre/factsheets/fs375/en/. Accessed October 11, 2016.
2. Frézard F, Demicheli C, Ribeiro RR. Pentavalent antimonials: new perspectives for old drugs. *Molecules*. 2009;14(7):2317–2336.
3. Alvar J, Vélez ID, Bern C, et al. Leishmaniasis worldwide and global estimates of its incidence. *PLoS One*. 2012;7(5):e35671. [Kirk M, editor].
4. Marsden PD. Mucosal leishmaniasis ("spundia" Escomel, 1911). *Trans R Soc Trop Med Hyg*. 1986;80(6):859–876.
5. World Health Organization. *Accelerating Work to Overcome the Global Impact of Neglected Tropical Diseases – A Roadmap for Implementation*. Geneva: WHO Press; 2012. Available from: http://whqlibdoc.who.int/hq/2012/WHO_HTM_NTD_2012.1_eng.pdf. Accessed October 11, 2016.
6. Berman JD, Waddell D, Hanson BD. Biochemical mechanisms of the antileishmanial activity of sodium stibogluconate. *Antimicrob Agents Chemother*. 1985;27(6):916–920.
7. Berman JD, Hanson WL, Lovelace JK, et al. Activity of purine analogs against *Leishmania donovani* in vivo. *Antimicrob Agents Chemother*. 1987;31(1):111–113.
8. Wyllie S, Cunningham ML, Fairlamb AH. Dual action of antimonial drugs on thiol redox metabolism in the human pathogen *Leishmania donovani*. *J Biol Chem*. 2004;279(38):39925–39932.
9. Jeddi F, Piarroux R, Mary C. Antimony resistance in leishmania, focusing on experimental research. *J Trop Med*. 2011;2011:1–15.
10. Marsden PD. Pentavalent antimonials: old drugs for new diseases. *Rev Soc Bras Med Trop*. 1985;18(3):187–198.
11. Gutiérrez V, Seabra AB, Reguera RM, Khandare J, Calderón M. New approaches from nanomedicine for treating leishmaniasis. *Chem Soc Rev*. 2016;45(1):152–168.
12. Prasad PN. *Introduction to Nanomedicine and Nanobioengineering*. Hoboken, NJ: John Wiley & Sons Inc; 2012.
13. Kaur IP, Kakkar V, Deol PK, Yadav M, Singh M, Sharma I. Issues and concerns in nanotech product development and its commercialization. *J Control Release*. 2014;193:51–62.
14. CLINAM. *The European Summit for Clinical Nanomedicine and Targeted Medicine. The Translation to Knowledge Based Medicine*. Available from: https://clinam.org/images/stories/pdf/conference2015.pdf. Accessed October 11, 2016.
15. Tripathy S, Roy S. A review of age-old antimalarial drug to combat malaria: efficacy up-gradation by nanotechnology based drug delivery. *Asian Pac J Trop Med*. 2014;7(9):673–679.
16. Prabhu P, Patravale V, Joshi M. Nanocarriers for effective topical delivery of anti-infectives. *Curr Nanosci*. 2012;8(4):491–503.
17. Moosavian Kalat SA, Khamesipour A, Bavarsad N, et al. Use of topical liposomes containing meglumine antimoniate (Glucantime) for the treatment of *L. major* lesion in BALB/c mice. *Exp Parasitol*. 2014;143(1):5–10.
18. Pham TTH, Loiseau PM, Barratt G. Strategies for the design of orally bioavailable antileishmanial treatments. *Int J Pharm*. 2013;454(1):539–552.
19. Grafov A, Grafova I, Franco AMR, Leskelä M. Leishmanicidal inorgano-organic nanohybrids, synthesis and application of the same. Patent BR 10 2013 029618 0.
20. Coles GC, Bauer C, Borgsteede FHM, et al. World association for the advancement of veterinary parasitology (W.A.A.V.P.) methods for the detection of anthelmintic resistance in nematodes of veterinary importance. *Vet Parasitol*. 1992;44(1–2):35–44.
21. Abe M, Ito T. Synthetic inorganic ion-exchange materials. X. Preparation and properties of so-called antimonic(V) acid. *Bull Chem Soc Jpn*. 1968;41(2):333–342.
22. Bajārs G, Lagzdons J, Petrovskis G. Solid proton electrolytes in electrochromic systems. In: Lusis A, editor. *Elektrokhromizm*. Riga: Latvian State University; 1987:51–66.
23. Novikov BG, Materova EA, Belinskaya FA. On the nature and stability of precipitated polyantimonic acids. *Russ J Inorg Chem*. 1975;20(6):1566–1572.
24. Dzimitrowicz DJ, Goodenough JB, Wiseman PJ. A.C. proton conduction in hydrous oxides. *Mater Res Bull*. 1982;17(8):971–979.
25. Vaivars GJ, Kleperis JJ, Lūsis AR. Study on antimonic acid hydrates obtained by sol method. *Russ J Electrochem*. 1992;28(10):1438–1443.
26. Roberts WL, McMurray WJ, Rainey PM. Characterization of the antimonial antileishmanial agent meglumine antimonate (glucantime). *Antimicrob Agents Chemother*. 1998;42(5):1076–1082.
27. Ebner F, Heller A, Rippke F, Tausch I. Topical use of dexpanthenol in skin disorders. *Am J Clin Dermatol*. 2002;3(6):427–433.
28. Bissett DL, Oblong JE, Goodman LJ. Topical vitamins. In: Draelos ZD, editor. *Cosmetic Dermatology: Products and Procedures*. 2nd ed. Wiley-Blackwell; 2015:336–345.